Journal of
Polymer Materials

Tech Science Press

Doi:10.32604/jpm.2026.076318

ARTICLE

Influence of Processing Route on the Mechanical Properties of Poly(Lactic Acid)-Poly(Caprolactone)-Basalt Fiber Composites Prepared via Planetary Extrusion

Declan Mary Colbert[1,*], Eyman Manaf[1], Zeeshan Ali[1], Steven Rowe[2], Chris Doran[2], Trevor Howard[2], Vlasta Chyzna[3], Evan Moore[3], Alan J. Murphy[3], Patrick Doran[4], Golnoosh Abdeali[1] and Declan M. Devine[1]

[1]PRISM Research Institute, Technological University of the Shannon, Athlone, Ireland
[2]Applied Polymer Technology Gateway, Technological University of the Shannon, Athlone, Ireland
[3]CISD, Technological University of the Shannon, Athlone, N37 HD68, Ireland
[4]Department of Polymer and Mechanical Engineering, Technological University of the Shannon, Athlone, Ireland

*Corresponding Author: Declan Mary Colbert. Email: declan.colbert@tus.ie

Received: 18 November 2025; Accepted: 12 January 2026; Published: 03 April 2026

ABSTRACT: A comparative analysis was performed on poly(lactic acid) (PLA), poly(caprolactone) (PCL), basalt fiber (BF) composites produced using two distinct approaches: direct blending and masterbatching. The limitations of PLA-BF composites with regard to distribution and adhesion are well-documented, as are chemical treatment methods (addition of compatibilisers, surface treatments, silanization). This work aimed to study an industrially relevant potential solution of utilising a PCL-BF masterbatch, prepared as a 50/50 wt.% blend using planetary roller extrusion (PEX) to both improve the distribution and homogeneity of the fibers as well as provide a secondary adhesion site to facilitate improved mechanical properties of the final PLA-PCL-BF composite. The resultant materials were injection moulded to prepare ISO standard test specimens and tested on the basis of their physical properties via tensile testing, impact strength testing, flexural analysis, Fourier transform infrared spectroscopy and water absorption capability. The results displayed that the incorporation of PCL and BF led to an increase in ductility of the composite materials, allowing for improvements in the inherent brittleness of virgin PLA. Major increases in the impact strength were achieved with the utilisation of a 25% PCL/BF masterbatch, allowing for a greater than 50% increase. As an overall observation, the use of a masterbatching process, opposed to direct blending of the constituent materials allows for a greater consistency of composite to be achieved at the expense of increased gains.

KEYWORDS: PLA; natural fibers; composites; planetary extrusion

1 Introduction

Though poly(lactic acid) (PLA) is often considered to be a promising, more sustainable replacement for conventional petroleum plastics, it is not without its drawbacks. The wide applicability of PLA lies in its similarity to commercially available petroleum polymers (polystyrene, polypropylene, poly(ethylene terephthalate)) with respect to its mechanical, thermal, barrier and optical properties [1], while having its constituent monomers derived from renewable plant sources such as sugar and starch [2]. Though these properties lend credence to PLA being a direct replacement material, two major limitations of PLA lie in its comparative lack of thermal stability, low flexibility and relative fragility, being quite brittle in nature [1,3].

To improve the mechanical performance of PLA-based materials, reinforcement with natural fibers (NFs) continues to be shown as a promising strategy. NFs are derived from sources of natural origin, i.e., plant-, animal- or mineral-derived [4]. With the current focus on increasing the sustainability of materials, the use of NFs as a reinforcement material in polymer composites has become an increasingly popular technique for various applications [5]. These NFs offer several benefits, such as low weight, low cost, biodegradability, while offering excellent mechanical properties [4,6–8] and pose as a potential replacement material for synthetic fibers [9]. The beneficial aspects of fiber reinforcement are tied to achieving a homogenous distribution of the fibers within the polymer matrix. Non-uniformities during the production of fiber-reinforced composites, such as clustering/agglomeration, fiber settlement and other forms of segregation may impede these beneficial aspects [10] and instead act as faults in the final composite. Basalt fiber (BF) has increasingly been viewed with interest within the field of fiber-based composites owing to its strength and stiffness as well as its thermal and chemical resistance [11]. Despite these potential improvements, the challenge remains of poor interfacial adhesion between the BF and PLA matrix caused by the hydrophobicity of the PLA and chemical inertness of the BF. This incompatibility limits effective stress transfer within the PLA-BF composite, thus resulting in below optimal mechanical properties [12–14]. Numerous strategies have been published to improve the interfacial adhesion between PLA and BF, such as silanization [15,16], of coupling agent [17], surface assembly with *in-situ* SiO_2 nanoparticles [18] and surface treatment of the BF with atmospheric pressure glow discharge plasma [19]. Though the incorporation of BF into a PLA matrix has been shown to improve the mechanical properties of the PLA, its brittle nature remains a challenge. The most efficient method of improving the mechanical brittleness of a polymer is through melt blending with a softer more ductile polymer [20]. Poly(caprolactone) (PCL), a biodegradable aliphatic polyester, is a flexible polymer that similar to PLA, has found significant interest in the biomedical space owing to its long *in vivo* degradation rate [21] and biocompatibility [22].

The choice of processing technique is an important criterion in determining the distribution of fibers, orientation and ability to retain fiber length, factors that influence the overall properties of the final composite. Twin-screw extrusion (TSE), particularly co-rotating extrusion, is known to provide significantly better mixing capabilities compared to single-screw extrusion (SSE). However, the intense shear action is known to lead to fiber breakage and result in a decrease in fiber length. This reduction may be such that the final composite fibers have been reduced to a number of micrometres regardless of the original starting fiber length [23]. Our previous work has shown that when using both conical [24] and parallel extrusion [25] fiber breakage remained a significant issue. Similarly, Kryszak et. al prepared composite material via melt extrusion and injection moulding. This work quantitatively analysed the particle size distributions of hydroxyapatite and noted a significant reduction in the amount of larger grains, also posited as due to the significant thermal and mechanical stresses imparted within the extrusion process [26].

Planetary roller extruders, due to their characteristic configuration, allow for excellent dispersive mixing using lesser shear forces and as such, may provide applicability in both achieving uniform distribution of fibers, while preventing agglomeration and fiber breakage [27]. Due to the relative lack of laboratory-scale planetary extrusion equipment, TSE continues to be the predominantly focused on technique with regards to academic literature with the term “twin screw extruder” yielding 77% of Google Scholar hits, “single screw extruder” yielding 22.9% while “planetary extruder” yields only 0.06% of hits. As such, planetary extrusion (PEX) represents a field of polymer processing that has to date been underserviced in the academic field [28] though presents numerous advantages over its single- or twin-screw counterparts. The configuration of a PEX, such as that shown in Fig. 1, allows for much greater contact surface than is feasible with either SSE or TSE. Formella and Eyigöz calculated that a PEX with a screw diameter of 165 mm and length of 1000 mm working at a screw speed of 50 rpm would provide 353 $m^2 \cdot min^{-1}$ of contact surface. For a TSE to obtain a

similar contact, the barrel length would need to be 40 times greater, while an SSE would need to be 140 times longer [28].

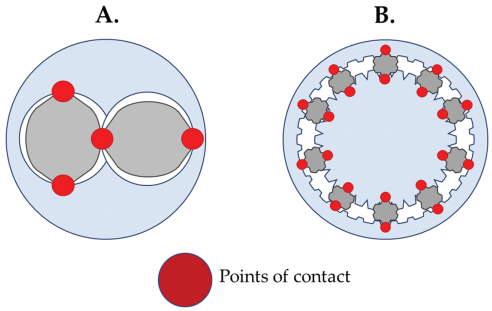

Figure 1: Points of contact in; (**A**) Twin-screw extruder (TSE) and (**B**) Planetary roller extruder (PRE)

The objective of this study was to attempt to overcome the mechanical limitations of PLA and the inherently poor adhesion between BF and PLA through the incorporation of PCL. This was performed through using a single mixed blend of the three constituent components and a comparative blend whereby an initial PCL/BF masterbatch was prepared prior to processing along with the PLA. The resultant 6 formulations were analyzed and compared on the basis of physicochemical and mechanical properties.

2 Materials and Methods

2.1 Materials

The PLA used for this study was Ingeo^{TM} Biopolymer 4043D supplied by Natureworks (*MN, United States of America*). Prior to processing the PLA was dried at 80°C for 4-h as per the suppliers' guidelines. The PCL used was CAPA 6800, supplied by Perstorp (*Malmö, Sweden*). Basalt fiber was supplied by Basaltex NV (*Wevelgem, Belgium*). The BF was supplied as a continuous fiber with a diameter of 14 μm and manually cut to a length of 25 mm by means of a rotary fiber cutter.

2.2 Blend Preparation

2.2.1 Masterbatch Preparation

A PCL-BF masterbatch was initially prepared as a 50/50 composition. The PCL and BF were accurately weighed and placed into polyethylene bags. The mags were manually tumble blended for 10-mins to ensure a homogenous distribution. The mixed material was fed into an ENTEX Planetary roller extruder (*Bochum, Germany*), consisting of a central spindle and 6 symmetrically balanced helical screws equipped with a twin-screw side feeding unit (Fig. 2). The feeding rate was adjusted to 100 rpm with an extrusion rotational speed of 130 rpm. The temperature of the extruder was maintained at 80°C throughout the 3 zones (Zone 1, Zone 2 and the Screw). The resultant material was cooled under pressurised air and pelletized to 3.0 mm in length using a Thermo Scientific pelletising unit (*MA, United States of America*).

2.2.2 Composite Preparation

The composition of the prepared composites is shown in Table 1. The ratio of the masterbatch (MB) was maintained so as to provide an equivalent loading percentage of BF as the non-processed blend. The non-processed blend consisted of PLA, PCL and BF undergoing extrusion without an initial MB preparation step. The feeding rate was adjusted to 80 rpm with an extrusion rotational speed of 130 rpm. The temperature profile was adjusted to 175°C at Zone 1 and Zone 2 while the Screw was maintained at 150°C.

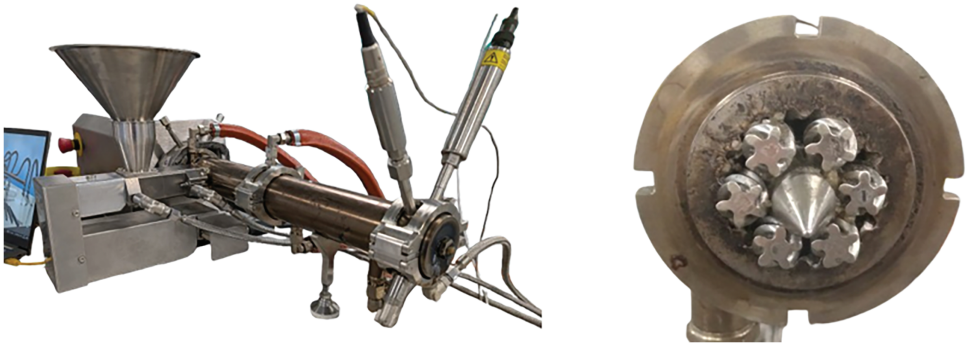

Figure 2: ENTEX planetary roller extruder and screw configuration

Table 1: Formulations prepared via planetary extrusion for this study

Sample ID	PLA (wt.%)	PCL (wt.%)	BF (wt.%)	MB (wt.%)
MB	–	50	50	–
A_1	100	–	–	
B_1	90	5	5	
B_2	75	12.5	12.5	
B_3	50	25	25	
C_1	90			10
C_2	75	–	–	25
C_3	50	–	–	50

2.3 Injection Moulding

Injection moulding of standard test specimens was carried out using an Arburg Allrounder 37A (*Loßburg, Germany*). The moulding parameters used are shown in Table 2. All materials were pre-dried for 4-h at 90°C prior to undergoing injection molding trials.

Table 2: Injection molding parameters for the preparation of test specimens

Parameter	Unit	Setting
Injection speed	mm/s	40
Injection pressure	Bar	900
Holding pressure	Bar	700
Switch over point	mm	12
Screw speed	mm/s	150
Back pressure	Bar	40
Shot size	mm	33
Cooling time	s	30
Zone 1	°C	170
Zone 2	°C	175
Zone 3	°C	180
Zone 4	°C	185
Nozzle	°C	190

(Continued)

Table 2 (continued)

Parameter	Unit	Setting
Mold temperature	°C	40

2.4 Tensile Testing

Tensile testing was performed in accordance with EN ISO 527 [29] standard for test specimens using an Zwick Roell tensile tester (*Ulm, Germany*) [29]. A total of 6 specimens for each sample were tested, with dimensions of 96 mm in length, a width of 13 ± 0.2 mm, and a thickness of 3 ± 0.2 mm. The tensile testing was performed under quasi-static conditions at a speed of 50 mm/min at ambient room temperature, approximately 20°C. The tensile properties were determined from the stress-strain data obtained during analysis with strain calculated from crosshead displacement. Youngs modulus was calculated from the initial linear elastic region of the stress-strain curve (0.05%–0.25%).

2.5 Flexural Testing

Flexural testing was conducted on Lloyd LRX Tensometer (*Hampshire, United Kingdom*) after conditioning for a minimum of 24 h at 23 ± 2°C. The Tensometer was fitted with a 2.5 kN loadcell and a 3-point bending jig. Experimental settings were in accordance with ISO 178 [30]. Six replicates were placed centrally across two rollers with a span of 96 mm and tested at a speed of 2 mm/min. Flexural strength was calculated using Eq. (1).

$$\partial f = \frac{3FL}{2bd^2} \tag{1}$$

where;

F = force at the point of fracture

L = support span length

b = width of the sample

d = depth of the sample

2.6 Impact Testing

A calibrated Zwick Roell CEAST 6545 (*Ulm, Germany*) was used to carry out a Charpy notched impact test in accordance with ISO 179-1 [31]. Test specimens, with an average thickness of 12.72 mm (±0.04 mm), were notched to a depth of 2.0 mm and then placed in the sample holder. A 4 J hammer attachment was used and initially zeroed by releasing the arm with no samples in the holder. The sample was then placed with the notch placed as centrally to the arm as possible. The hammer arm was then locked in the upward position and subsequently released. The resultant downswing of the arm provides the impact energy of the test specimen in J. The impact strength of samples was subsequently calculated using Eqs. (2) and (3), where K = notch impact energy, m = mass of hammer, g = gravity constant, A = cross-sectional area and $\propto$ = notch toughness.

$$K = m \times g \times (H - h) \tag{2}$$

$$\propto = \frac{K}{A} \tag{3}$$

2.7 Fourier Transform Infrared Spectroscopy

FTIR testing was conducted using a Thermo Scientific Nicolet™ iZ™10 FT-IR spectrometer (*Waltham, Massachusetts, United States*) with Smart iTX™ Attenuated Total Reflectance (ATR) accessory. Fourier transform infrared spectroscopy was carried out using the ATR mode of the FTIR with a 4-scan-per-sample cycle and a resolution of 8. The sample was scanned from 650 to 4000 cm^{-1}. During clamping, a pressure force of approximately 80 N was applied to ensure optimal contact between the sample and the diamond crystal.

2.8 Water Absorption

Water absorption (WA) of the prepared composite samples was carried out in accordance with ASTM D570-22 [32]. Injection moulded samples were first dried at 50°C for 24-h and accurately weighed (W_1). The samples were subsequently immersed in deionised water at 22°C for 30-days. Upon completion of this time, the samples were removed, blotted dry of surface moisture using filter paper and weighed (W_2). The WA of the samples was calculated using Eq. (4).

$$WA\,(\%) = \frac{W_2 - W_1}{W_1} \times 100 \tag{4}$$

2.9 Fracture Surface Morphology

The morphology of the fracture surface of injection-molded tensile bars was evaluated using a scanning electron microscope (*Tescan Mira, Oxford Instruments, Cambridge, UK*). Prior to imaging, samples were attached to an adhesive conducting tape on the stubs and subsequently sputtered with gold utilizing a Baltec SCD 005 sputter coater (*BAL-TEC GmbH, Schalksmühle, Germany*).

3 Results & Discussion

3.1 Tensile Properties

The characteristic tensile properties of the produced composite samples are shown in Table 3 with a comparison of the tensile strengths, with respect to percentage inclusion of combined reinforcement, shown graphically in Fig. 3. The highest tensile strength was displayed by sample A_1, the virgin PLA. This was followed by a sequential decreasing in tensile strength with respect to increasing proportion of PCL. This was expected as PCL is well-documented for its low tensile strength and tensile modulus [33]. The emphasis of incorporating the PCL within this work was not to improve the tensile properties of the composite to act as a flexibility and ductility enhancer. The samples B_1–B_3 all displayed a decrease in tensile strength, increase in tensile modulus and decrease in elongation at break with respect to the virgin PLA. These trends could all be rationalized on the basis of the increasing percentage of PCL (tensile strength) and basalt (tensile modulus and elongation at break) as well as the direct blending approach followed by these samples. The utilization of a direct blending approach, especially with fibers known to suffer from agglomeration at high loading levels, may lead to inadequate distribution of the PCL fraction within the PLA matrix as well as rick the localized formation of basalt agglomerates. The masterbatch samples (C_1–C_3) meanwhile would appear to benefit greatly from a much more homogeneous distribution of both the PCL and BF thus allowing for an improvement in tensile modulus and elongation at break compared to the virgin PLA. The observable trends herein show the balanced approach that needs to be undertaken with the masterbatching approach.

While greater gains are observed with the direct blending approach, a much greater degree of consistency is achievable when implementing a masterbatching strategy. Though in this work, a single planetary extrusion process was employed, further research may be performed with lower screw speeds owing to the distributive mixing allowable via PEX in order to retain fiber length throughout the process.

Table 3: Tensile properties of the PLA-PCL-BF composite samples. All values are shown ± the standard deviation. ε_t: Youngs Modulus; ε_{tB}: Elongation at break

Sample	Tensile strength (MPa)	ε_t (MPa)	ε_{tB} (%)
A_1	64.2 ± 0.5	2476.7 ± 28.3	5.7 ± 1.4
B_1	57.9 ± 0.8	2545.3 ± 59.1	5.0 ± 0.2
B_2	50.0 ± 0.6	2863.1 ± 42.1	4.5 ± 0.2
B_3	58.0 ± 0.5	2944.0 ± 25.3	3.5 ± 0.5
C_1	56.6 ± 0.6	2504.1 ± 18.1	8.1 ± 1.4
C_2	54.3 ± 0.8	2623.0 ± 19.8	6.3 ± 1.1
C_3	45.2 ± 0.4	2630.8 ± 40.9	5.9 ± 0.6

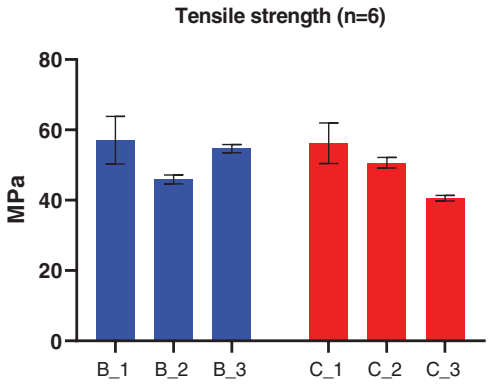

Figure 3: Comparison of tensile strength (n = 6) between direct blended (blue) and masterbatched (red) composites

3.2 Impact Strength

The results of impact strength analysis including impact strength and percentage increase compared to the virgin PLA are shown in Table 4. With regards to virgin PLA, the primary mechanical drawback is well-documented to be its brittle mode of failure and lack of impact strength [34,35]. Though fiber reinforcement of polymer composites is a well-regarded practice for the improvement of impact properties, the selection of reinforcement requires careful consideration as previous authors have shown that certain fibers have a deleterious effect on impact strength of PLA composites. Graupner et al. showed that PLA composites reinforced with hemp fibers or kenaf fibers, produced via compression molding led to a decrease in impact strength of 58% and 63%, respectively [36]. Bax and Müssig meanwhile developed composites of PLA and flax fibers produced via injection moulding, arising in a 31% decrease in impact strength [37]. Similarly the work by Huda et al. employing wood fibers to create injection molded PLA composites yielded a 13% decrease in impact strength [38]. As can be seen in Table 4, the incorporation of BF and PCL are in stark contrast to these previously published bodies of work. Reinforcement of the composites produced in this study benefit not only from the high stiffness of the included BF, but so too from the inclusion of the ductile secondary polymer, PCL. As such there is a dual-reinforcement effect with respect to the two additives. Though at low

and high-levels of reinforcement, the direct blended samples (B_1 & B_3) and masterbatch-based samples (C_1 & C_3) yield similar increases in impact strength (14.64%/15.18% and 51.17%/54.82%, respectively). Conversely, at intermediary loading levels of PCL/BF, the direct blending approach yielded a more than doubled increase in impact strength (65.39% compared to 30.45%). The utilization of BF as a PLA impact enhancer is well-known though the additional inclusion of PCL into the matrix significantly improves upon this effect. Notably, Kuciel et al. demonstrated that at a 15% loading level of BF, an increase in impact strength of 26.6% was obtained [39]. Within this study, when utilizing a similar but lesser loading level of BF and a similar loading of PCL (12.5%) this increase in impact strength is greatly improved upon with direct blending displaying a 65.39% increase and masterbatching displaying a 30.45% increase.

Table 4: Determined impact strength of the PLA-PCL-BF composites

Sample	Impact strength (kJ/m²)	Std. Dev.
A_1	4.5	0.2
B_1	5.3	0.4
B_2	13.0	1.3
B_3	9.2	1.3
C_1	5.3	0.4
C_2	6.5	1.0
C_3	10.0	1.0

Fig. 4 displays a comparison of the increase in impact strength compared to the virgin PLA sample. Contextualizing the data in this manner as opposed to just observing the highest and lowest values clearly demonstrates the potential value to be gained from the masterbatching approach. Though the direct blending approach yielded the highest gain in impact strength (B_2), there is no discernible trend with regards to higher loading levels. Numerous authors have posited that at higher loading levels there is an inherently higher risk of causing agglomeration of the fibers and subsequently the fibers act as weak spots instead of reinforcements [40].

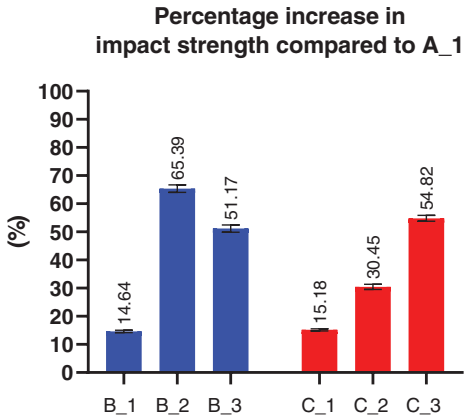

Figure 4: Percentage increase in impact strength compared to virgin PLA (A_1). blue bars denote the direct blended composites, red bars denote Masterbatched composites

3.3 Flexural Strength

The results for flexural analysis of the composite samples are shown in Table 5 and Fig. 5. As can be seen the highest flexural strength again is shown by the virgin PLA (A_1). As PLA is widely known for its high stiffness and brittle nature, this was to be expected [41]. The effect of incorporating increasing proportions of PCL is readily apparent with a clear decrease in both Youngs modulus of bending and flexural strength with respect to increasing PCL content. This shows the additive effect on the ductility of the composite allowed by the incorporation of the very ductile PCL.

Table 5: Results of flexural analysis (3-point bend) for the direct blended (B_1–B_3) and masterbatched (C_1–C_3) composites

Batch	Young's Modulus of Bending (MPa)	% Change	Flexural Strength (MPa)	% Change
A_1	2076.1 ± 24.3	–	83.40 ± 0.97	–
B_1	2104.0 ± 31.0	+1.3	74.5 ± 1.3	−10.7
B_2	2531.8 ± 61.5	+22.0	61.6 ± 1.1	−26.2
B_3	2248.2 ± 119.6	+8.3	69.1 ± 2.1	−17.2
C_1	2032.5 ± 33.9	−2.1	70.6 ± 0.8	−15.4
C_2	2084.6 ± 50.4	+0.4	65.6 ± 0.6	−21.3
C_3	2148.0 ± 62.3	+3.5	53.9 ± 0.8	−35.4

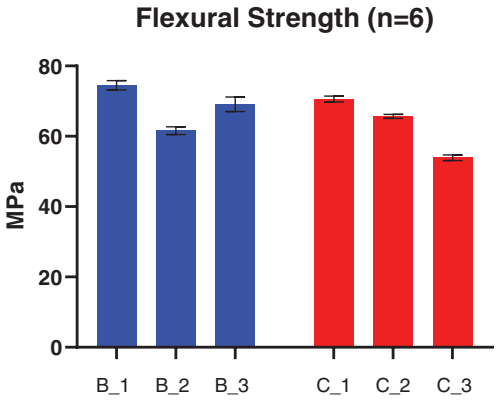

Figure 5: Comparison of the flexural strength of direct blended (blue) and masterbatched (red) composites

Amongst the direct blended samples (B_1–B_3), there is a sharp increase in Youngs Modulus with sample B_2 showing the greatest value (2531.8 MPa). Such behaviour indicates that at intermediate PCL content the composite exhibits a temporary stiffening effect. Despite this increase in modulus, all B samples show a reduction in flexural strength relative to 100% PLA. The disassociation of strength and modulus suggests that bending stiffness may increase at certain blend ratios but the increasing proportion of ductile PCL phase reduces the composites' ability to sustain maximum bending stress. The direct blended composites thereby result in a higher degree of ductility that fail at lower applied flexural loads, consistent with typical behaviour observed in PLA/PCL systems [42,43].

For the composites prepared via masterbatching (C_1–C_3), a consistent decreasing trend is observed in flexural strength is observed with sample C_3 showing a 35.36% reduction in flexural strength compared to virgin PLA (A_1). The values for Youngs Modulus, however, remain closer aligned to that of A_1. This

may suggest that the masterbatching approach facilitated better dispersion of the polymeric phases as well as the fibers preventing localized agglomeration thus preserving stiffness at the sacrifice of flexural strength. The overall decrease in both Modulus and Flexural strength is primarily caused by the natural ductility of the PCL allowing the composites to bend with lesser force applied, as discussed by Chee et al. [44].

3.4 Composite Infrared Spectra

The FTIR spectra of PLA-PCL-BF and PLA-MB composites are shown in Fig. 6. The IR spectra display a lack of chemical interaction between the three components of the composite samples, as expected. The presence of PLA is confirmed by the observation of peaks corresponding to CH_3, C=O and C-O while the presence of PCL is indicated by the presence of C-O, C=O and CH_2. The CH_2 peak of the PCL was observed at 2918.85 cm^{-1}, the C=O 1723.18 cm^{-1} and the C-O at 1106.38 cm^{-1}. The PLA meanwhile presented peaks at 1746.65, 2994.52 and 1080.20 cm^{-1} for the C=O, CH_3 and C-O, respectively. In the case of all of the composite samples, regardless of processing route utilized (direct blending or masterbatching), the spectra obtained were a sum of the constituent components with no appearance of new peaks indicating the components mix mechanically but not chemically [42,45,46]. Comparison of the spectra reveal subtle variations in the peak intensities within the composite samples primarily a decreasing intensity in the peak identified at ~1720 cm^{-1}. A similar result was obtained by [42,47] whom noted interaction via hydrogen bonding between the C=O group of the PLA with the -OH group of the PCL. Similarly, the CH_2 stretch of the PCL (~2919 cm^{-1}) shows slight broadening in intensity in the MB processed samples, possibly indicative of greater distribution of the PCL within the PLA-rich phase. No quantifiable major peak shifts were detected confirming that the components interact primarily through physical contact rather than via chemical bonding [44]. Though no new chemical bonds were formed within the spectra, the improvement in mechanical performance can be attributed to enhanced physical interactions of the individual components [48]. A greater uniformity in PCL and BF distribution increases the available interfacial contact area allowing for more efficient stress transfer between phases [20,42,49]. The presence of PCL also promotes greater fiber wetting of the BF surface, facilitating improved mechanical interlocking even without the presence of covalent bonding.

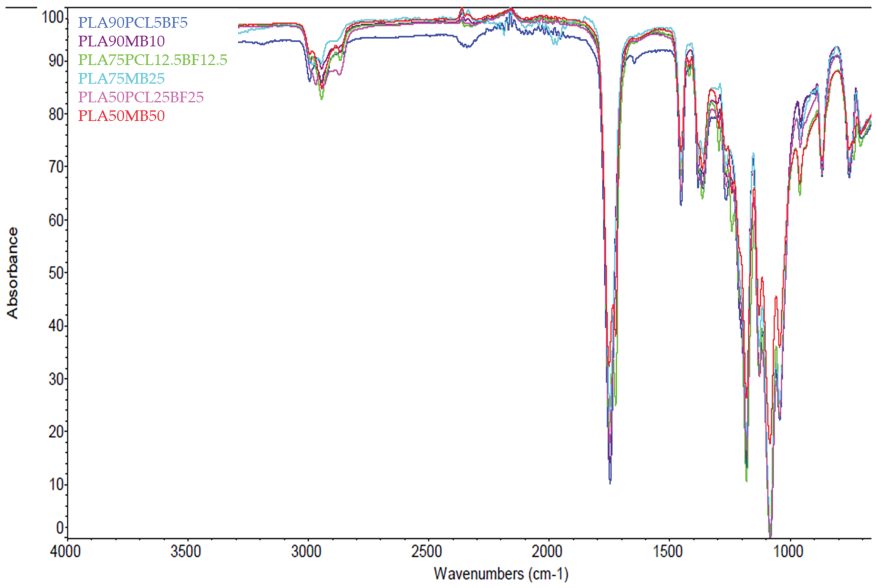

Figure 6: Overlay spectra of the PLA-PCL-BF and PLA-MB composites

3.5 Fracture Surface Morphology

Figs. 7–9 display SEM micrographs taken of the cross-sectional area of samples post-tensile testing in order to visually analyze interfacial adhesion and fiber distribution based on the two processing methods utilized. Fig. 7 compares the composites prepared at the lowest reinforcement loading, i.e., 10 wt.% total inclusion. The images labelled 1a and 1b are PLA90PCL5BF5, respectively, while 2a and 2b present PLA90MB10. The direct blended sample (1a and 1b) displays a homogenous matrix with the presence of distinct voids and fibers scattered across the fractured surface showing clear signs of fiber pull-out and interfacial debonding. These are indicative features of poor interfacial adhesion, a known phenomenon between PLA and BF when there is no addition of a chemical coupling agent commonly maleic anhydride [50], as discussed in our previous works [24,25]. In comparison, samples 2a and 2b (PLA90MB10) present a much greater distributive network of fibers within the surrounding matrix with no presentation of fiber debonding.

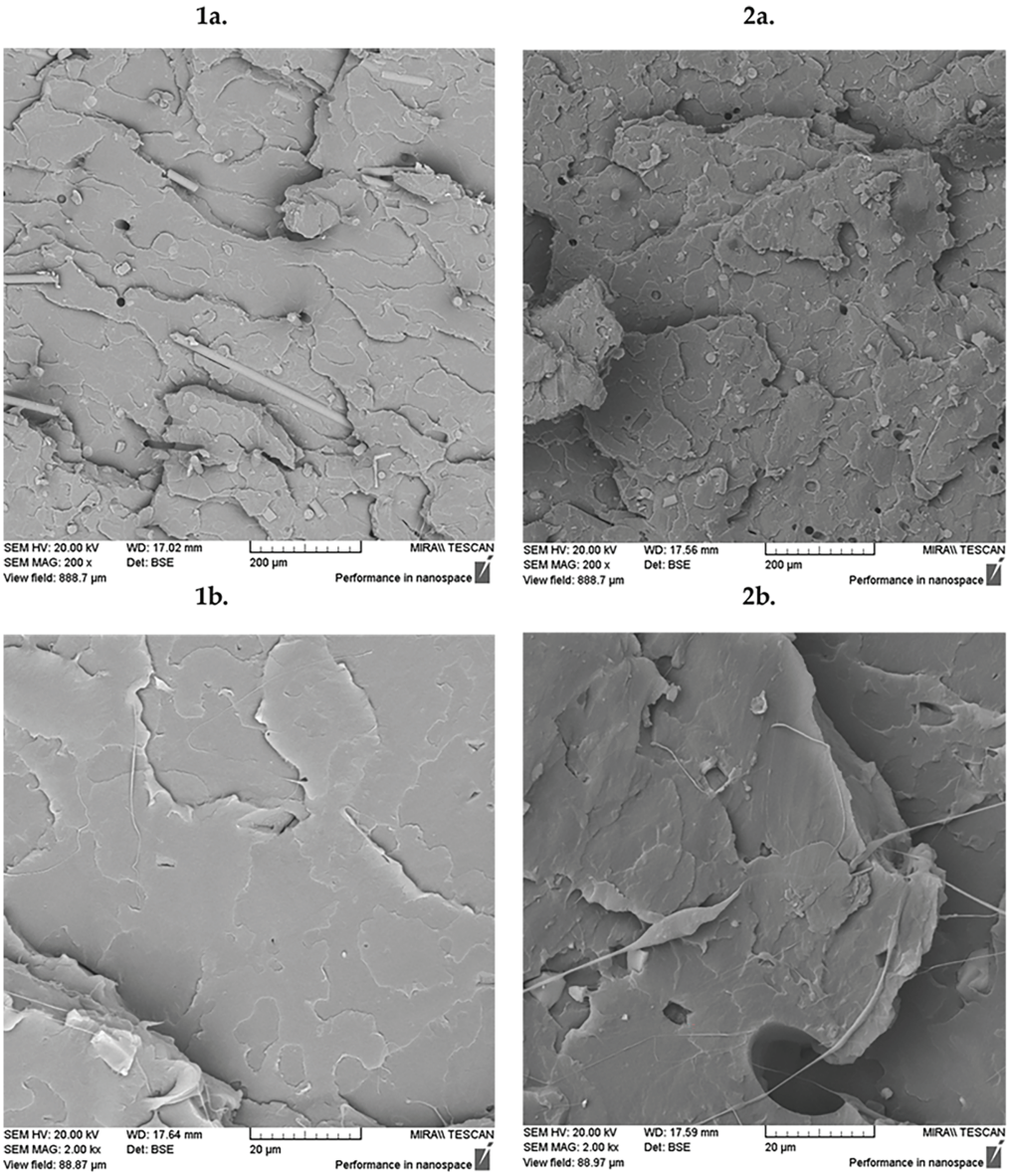

Figure 7: SEM micrograph displaying **1**. B_1 and **2**. C_1. Captioning "**a**" & "**b**" are indicative of 200× and 2000× magnification, respectively

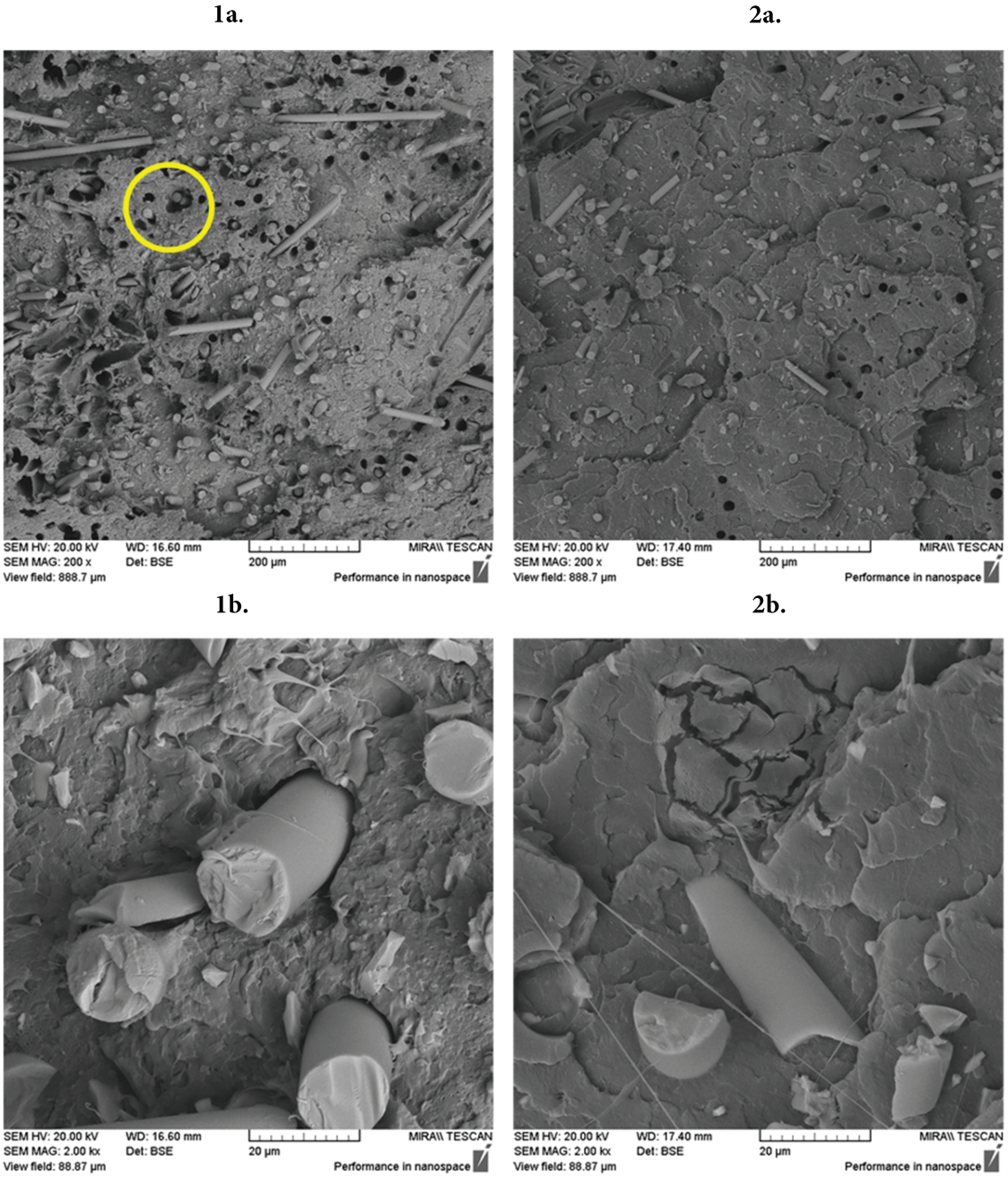

Figure 8: SEM micrograph displaying **1**. B_2 and **2**. C_2. Captioning "**a**" & "**b**" are indicative of 200× and 2000× magnification, respectively. Yellow circle indicates are of fiber agglomeration

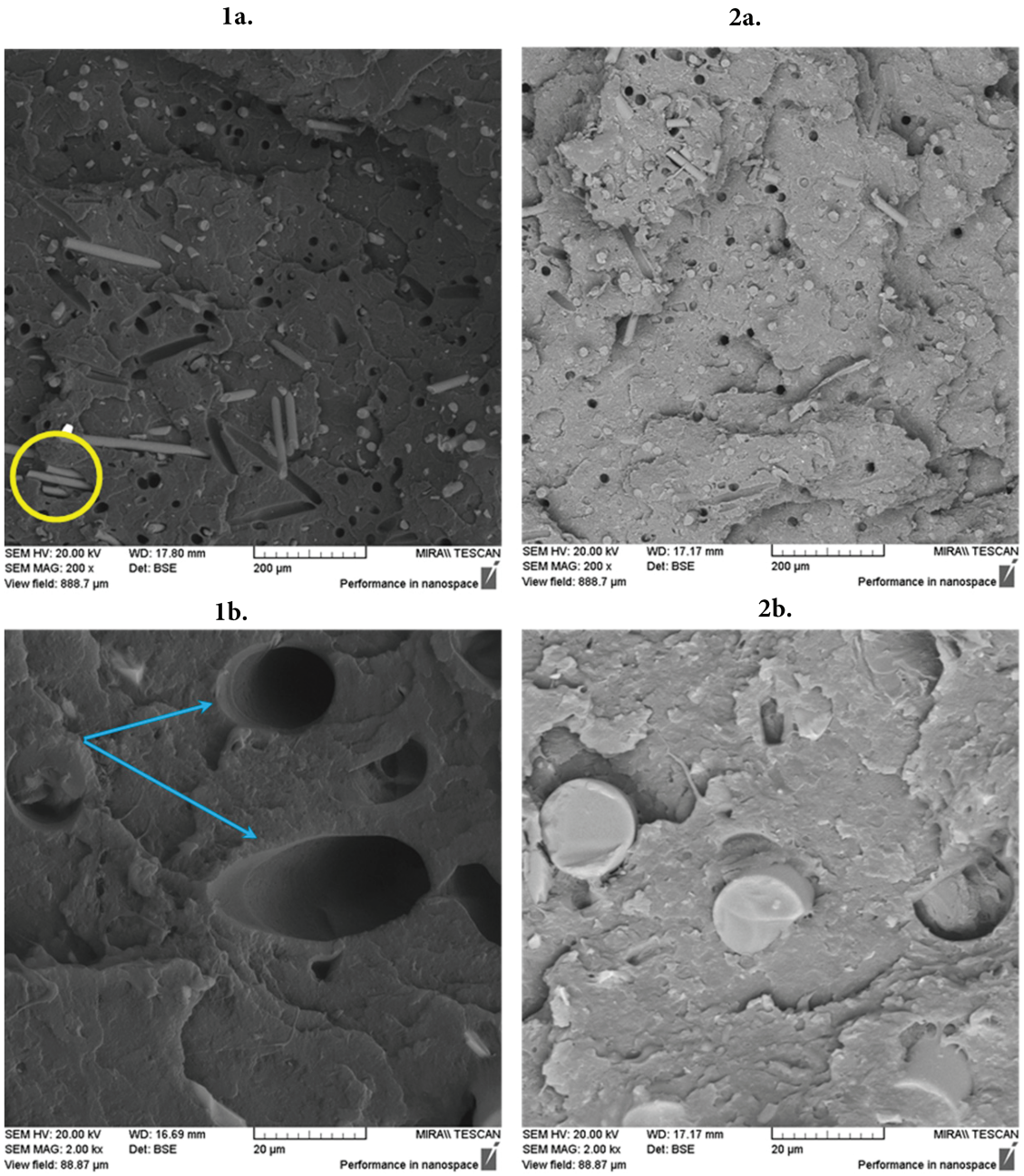

Figure 9: SEM micrograph displaying **1**. B_3 and **2**. C_3. Captioning "**a**" & "**b**" are indicative of 200× and 2000× magnification, respectively. Yellow circle indicates area of fiber agglomeration with blue arrows highlighting fiber pull-out

Fig. 8 presents the intermediate reinforcement level, namely PLA75PCL12.5BF12.5 (1a and 1b) and PLA75MB25 (2a and 2b). Within the direct blended sample, there is widespread appearance of fiber agglomeration, as shown in the region highlighted within a yellow circle. The agglomeration is evident when coupled with the poor interfacial adhesion leading to non-symmetrical voids greater than the outer diameter of the fibers. Again, the distribution of fibers and lack of agglomeration is readily evident within the masterbatch prepared samples while the fracture morphology of the surrounding matrix appears much

more rounded indicating a more ductile failure mechanism than that of the much more jagged direct blended sample. The 2000× image lends credence to the masterbatching approach leading to improved adhesion between the surrounding matrix and fiber. As can be seen in 3b, the residual fiber remaining within the matrix displays a significant gap between the outer surface of the fiber and the matrix, whereas in 4b this gap is non-existent, indicating a greater degree of fiber-matrix adherence.

Fig. 9 presents the highest loading of reinforcement, 50% of the total material. Within this image, the previously mentioned issues of fiber agglomeration, fiber pull-out and interfacial debonding are greatly pronounced. At 2000× magnification the fiber pull-out is to such an extent that there are fibers or fiber residue present (blue arrow) indicating the fibers failed to adhere to the surrounding matrix. In contrast, the PLA50MB50 sample displays fibers that are well-embedded into the surrounding matrix. Though there are voids present, their symmetrical morphology is evidence of the absence of significant fiber agglomeration.

Though the samples prepared via the masterbatch approach showed much better dispersion, uniformity and improved interfacial adhesion, it is of importance to note that there is a greater degree of fiber breakage and fracture when compared to the direct blended approach. This is a limitation of the work performed whereby a single masterbatch was prepared at a relatively high screw speed to ensure uniform mixing of the fibers. Further studies with similar formulations but a lower rotational speed coupled with the mixing capabilities of the PEX may be sufficient to negate these issues. While the SEM images provide clear qualitative evidence of differences in fiber dispersion, interfacial adhesion, and breakage between the two processing routes, no quantitative assessment of fiber length distribution, void ratios, or fiber pull-out dimensions was performed in this study. Tensile fracture surfaces inherently introduce sampling bias, as local deformation fields influence fiber orientation, degree of pull-out, and crack propagation behaviour, making them unsuitable for reliable statistical measurement. Moreover, the focus of this work was on comparing the overall processing influence of direct blending vs. masterbatching rather than conducting a full morphological quantification. Future studies will employ controlled sample preparation and standardized imaging protocols to enable accurate quantitative analysis of fiber geometry and dispersion.

3.6 Water Absorption Capacity

The comparison of water uptake of the virgin PLA and PLA-based composites over a 30-day period is show in Table 6. As PLA is often presented as an advantageous bioplastic for packaging applications, it is important that the modification or inclusion of additional materials does not significantly impact on the inherent hydrophobic nature of the PLA. Owing to both PCL and BF being hydrophobic in nature, composite materials of the three should in turn display a similar degree of hydrophobicity.

Table 6: Water absorption capacity of the PLA-BF-PCL composite samples. σ: standard deviation

Sample	%WA	σ
A_1	0.72	0.18
B_1	0.82	0.10
B_2	0.67	0.09
B_3	0.66	0.28
C_1	0.56	0.18
C_2	0.64	0.06
C_3	0.83	0.03

Virgin PLA (A_1) absorbed 0.72% ± 0.18% over the 30-day submersion time, a low level of absorption consistent with its hydrophobic nature. Amongst the direct blended samples, sample B_1 (PLA90PCL5BF5) showed a mild increase in water uptake (0.82% ± 0.10%) potentially due to the formation of microvoids at lower filler levels or a result of fiber agglomeration during the processing [51]. With increasing filler levels, however the water uptake decreased to 0.67% ± 0.09% and 0.66% ± 0.28% for B_2 and B_3, respectively. Li et al. similarly examined the effect of incorporating PCL into PLA/PCL melt-blended films with an increased affinity to water displayed by contact angle. Similarly, to the water uptake results showed herein (i.e., a minor increase in hydrophilicity) the authors posited that the melt mixing of PCL and PLA leads to a greater presence of more polar (carbonyl) groups within the system, thus accelerating the absorption of water [52].

4 Conclusions

This study offered a comprehensive investigation regarding the influence of processing methodology (direct blending vs. masterbatch preparation) on the mechanical properties of PLA-based composites dually reinforced with PCL and BF. Though both routes demonstrate the potential to alleviate the inherent brittleness of PLA, the masterbatching approach yields greater fiber dispersion, improves interfacial adhesion and presents a more homogenous fracture morphology, resulting in greater consistency across the entirety of mechanical properties. Though the direct blended approach yielded higher peak values in some instances, the irregularity of formulations reinforces the challenges posed by fiber agglomeration and poor interfacial adhesion. SEM imaging displayed improved fiber-matrix adhesion in masterbatched samples, while the water absorption capacity displays slight increases when compared to virgin PLA, indicating retention of the hydrophobic properties. In essence, masterbatching presents a more industrially relevant and reproducible approach to manufacturing PLA-PCL-BF composites with improved toughness and ductility. From an industrial standpoint, PEX offers several advantages that complement the masterbatching approach. PEX systems allow high throughput, highly distributive mixing and efficient heat transfer with comparatively low shear stresses, making them well-suited to fiber-reinforced composite compounding where maintenance of fiber integrity is crucial. Though shortening of the fibers was observed in this study, further optimisation of processing parameters may help alleviate fiber damage with enhancement of mechanical performance.

Acknowledgement: Not applicable.

Funding Statement: The authors received no specific funding for this study.

Author Contributions: The authors confirm contribution to the paper as follows: Conceptualization, Declan Mary Colbert; methodology, Declan Mary Colbert, Eyman Manaf, Zeeshan Ali, Patrick Doran, Chris Doran, Trevor Howard and Evan Moore; formal analysis, Declan Mary Colbert, Steven Rowe, Golnoosh Abdeali and Patrick Doran; investigation, Declan Mary Colbert, Zeeshan Ali, Golnoosh Abdeali and Vlasta Chyzna; resources, Patrick Doran and Steven Rowe; data curation, Declan Mary Colbert; writing—original draft preparation, Declan Mary Colbert; writing—review and editing, Declan Mary Colbert and Declan M. Devine; visualization, Declan Mary Colbert and Vlasta Chyzna; supervision, Alan J. Murphy and Declan M. Devine; project administration, Declan M. Devine. All authors reviewed and approved the final version of the manuscript.

Availability of Data and Materials: The authors confirm that the data supporting the findings of this study are available within the article.

Ethics Approval: Not applicable.

Conflicts of Interest: The authors declare no conflicts of interest to report regarding the present study.

References

1. Khouri NG, Bahú JO, Blanco-Llamero C, Severino P, Concha VOC, Souto EB. Polylactic acid (PLA): properties, synthesis, and biomedical applications—a review of the literature. J Mol Struct. 2024;1309(3):138243. doi:10.1016/j.molstruc.2024.138243.
2. Shekhar N, Mondal A. Synthesis, properties, environmental degradation, processing, and applications of polylactic acid (PLA): an overview. Polym Bull. 2024;81(13):11421–57. doi:10.1007/s00289-024-05252-7.
3. Murariu M, Dubois P. PLA composites: from production to properties. Adv Drug Deliv Rev. 2016;107:17–46. doi:10.1016/j.addr.2016.04.003.
4. Feng Y, Hao H, Lu H, Chow CL, Lau D. Exploring the development and applications of sustainable natural fiber composites: a review from a nanoscale perspective. Compos Part B Eng. 2024;276(6414):111369. doi:10.1016/j.compositesb.2024.111369.
5. Hassanzadeh S, Hasani H. A review on milkweed fiber properties as a high-potential raw material in textile applications. J Ind Text. 2017;46(6):1412–36. doi:10.1177/1528083715620398.
6. Amiandamhen SO, Meincken M, Tyhoda L. Natural fibre modification and its influence on fibre-matrix interfacial properties in biocomposite materials. Fibres Polym. 2020;21(4):677–89. doi:10.1007/s12221-020-9362-5.
7. Ramamoorthy SK, Skrifvars M, Persson A. A review of natural fibers used in biocomposites: plant, animal and regenerated cellulose fibers. Polym Rev. 2015;55(1):107–62. doi:10.1080/15583724.2014.971124.
8. Westman MP, Fifield LS, Simmons KL, Laddha S, Kafentzis TA. Natural fiber composites: a review. Richland, WA, USA: Pacific Northwest National Lab; 2010. doi:10.2172/989448.
9. Khalid MY, Arif ZU, Sheikh MF, Ali Nasir M. Mechanical characterization of glass and jute fiber-based hybrid composites fabricated through compression molding technique. Int J Mater Form. 2021;14(5):1085–95. doi:10.1007/s12289-021-01624-w.
10. Bolander JE, Choi S, Duddukuri SR. Fracture of fiber-reinforced cement composites: effects of fiber dispersion. Int J Fract. 2008;154(1):73–86. doi:10.1007/s10704-008-9269-4.
11. Dhand V, Mittal G, Rhee KY, Park SJ, Hui D. A short review on basalt fiber reinforced polymer composites. Compos Part B Eng. 2015;73(3):166–80. doi:10.1016/j.compositesb.2014.12.011.
12. LIUa SQ, Yu JJ, Wu GH, Wang P, Liu MF, Zhang Y, et al. Effect of silane KH550 on interface of basalt fibers (BFs)/poly (lactic acid) (PLA) composites. Ind Textila. 2019;70(5):408–12. doi:10.35530/it.070.05.1596.
13. Wang GJ, Liu YW, Guo YJ, Zhang ZX, Xu MX, Yang ZX. Surface modification and characterizations of basalt fibers with non-thermal plasma. Surf Coat Technol. 2007;201(15):6565–8. doi:10.1016/j.surfcoat.2006.09.069.
14. Girgin ZC, Yıldırım MT. Usability of basalt fibres in fibre reinforced cement composites. Mater Struct. 2016;49(8):3309–19. doi:10.1617/s11527-015-0721-4.
15. Ali Ermeydan M, Aykanat O, Altın Y. Preparation and characterization of hybrid PLA biocomposites reinforced by wood and silane treated basalt fibers or compatibilized by maleic anhydride-grafted polypropylene (MAPP). Polym Compos. 2024;45(11):9831–44. doi:10.1002/pc.28442.
16. King FL, Arul Jeya Kumar A, Vijayaragahavan S. Mechanical characterization of polylactic acid reinforced bagasse/basalt hybrid fiber composites. J Compos Mater. 2019;53(1):33–43. doi:10.1177/0021998318780208.
17. Ying Z, Wu D, Zhang M, Qiu Y. Polylactide/basalt fiber composites with tailorable mechanical properties: effect of surface treatment of fibers and annealing. Compos Struct. 2017;176:1020–7. doi:10.1016/j.compstruct.2017.06.042.
18. Hou X, Yao S, Wang Z, Fang C, Li T. Enhancement of the mechanical properties of polylactic acid/basalt fiber composites via *in-situ* assembling silica nanospheres on the interface. J Mater Sci Technol. 2021;84:182–90. doi:10.1016/j.jmst.2021.02.001.
19. Kurniawan D, Kim BS, Lee HY, Lim JY. Atmospheric pressure glow discharge plasma polymerization for surface treatment on sized basalt fiber/polylactic acid composites. Compos Part B Eng. 2012;43(3):1010–4. doi:10.1016/j.compositesb.2011.11.007.
20. Fortelny I, Ujcic A, Fambri L, Slouf M. Phase structure, compatibility, and toughness of PLA/PCL blends: a review. Front Mater. 2019;6:206. doi:10.3389/fmats.2019.00206.
21. Lam CXF, Hutmacher DW, Schantz JT, Woodruff MA, Teoh SH. Evaluation of polycaprolactone scaffold degradation for 6 months *in vitro* and *in vivo*. J Biomed Mater Res A. 2009;90(3):906–19. doi:10.1002/jbm.a.32052.

22. Gandha P, Surve T, Kandasubramanian B. 15—polycaprolactone as biomaterial. In: Mozafari M, Singh Chauhan NP, editors. Handbook of polymers in medicine. Cambridge, UK: Woodhead Publishing; 2023. p. 425–43. doi:10.1016/B978-0-12-823797-7.00015-0.
23. Zhuang H, Pu R, Zong Y, Dai GC. Relationship between fiber degradation and residence time distribution in the processing of long fiber reinforced thermoplastics. Express Polym Lett. 2008;2(8):560–8. doi:10.3144/expresspolymlett.2008.68.
24. Finnerty J, Rowe S, Howard T, Connolly S, Doran C, Devine DM, et al. Effect of mechanical recycling on the mechanical properties of PLA-based natural fiber-reinforced composites. J Compos Sci. 2023;7(4):141. doi:10.3390/jcs7040141.
25. Chyzna V, Rowe S, Finnerty J, Howard T, Doran C, Connolly S, et al. Effect of screw configuration on the recyclability of natural fiber-based composites. Fibers. 2025;13(7):98. doi:10.3390/fib13070098.
26. Kryszak B, Zarei M, Biernat M, Szterner P, Pagacz J, Tymowicz-Grzyb P, et al. Effect of hydroxyapatite size on properties of PBS-DLS/HAp composites obtained by twin-screw extrusion and injection moulding techniques. Compos Sci Technol. 2025;261:111039. doi:10.1016/j.compscitech.2025.111039.
27. Markarian J. Wood-plastic composites: current trends in materials and processing. Plast Addit Compd. 2005;7(5):20–6. doi:10.1016/S1464-391X(05)70453-0.
28. Formela K, Eyigöz B. Planetary roller extruders in the sustainable development of polymer blends and composites—past, present and future. Express Polym Lett. 2024;18(4):441–58. doi:10.3144/expresspolymlett.2024.32.
29. ISO 527-1:2019. Plastics—determination of tensile properties. Geneva, Switzerland: International organization for standardization (ISO); 2019.
30. ISO 178:2019. Plastics—determination of flexural properties. Geneva, Switzerland: International organization for standardization (ISO); 2019.
31. ISO 179-1:2023. Plastics—determination of Charpy impact properties. Geneva, Switzerland: International organization for standardization (ISO); 2023.
32. ASTM D570-22. Standard test method for water absorption of plastics. West Conshohocken, PA, USA: American Society for Testing and Materials; 2022.
33. Hashim HB, Emran NAAB, Isono T, Katsuhara S, Ninoyu H, Matsushima T, et al. Improving the mechanical properties of polycaprolactone using functionalized nanofibrillated bacterial cellulose with high dispersibility and long fiber length as a reinforcement material. Compos Part A Appl Sci Manuf. 2022;158(6):106978. doi:10.1016/j.compositesa.2022.106978.
34. Kuru Z, Kaya MA. Poly(lactic acid)/polyester blends: review of current and future applications. EJRnD. 2023;3(1):175–99. doi:10.56038/ejrnd.v3i1.259.
35. Fernández-Tena A, Otaegi I, Irusta L, Sebastián V, Guerrica-Echevarria G, Müller AJ, et al. High-impact PLA in compatibilized PLA/PCL blends: optimization of blend composition and type and content of compatibilizer. Macromol Mater Eng. 2023;308(12):2300213. doi:10.1002/mame.202300213.
36. Graupner N, Herrmann AS, Müssig J. Natural and man-made cellulose fibre-reinforced poly(lactic acid) (PLA) composites: an overview about mechanical characteristics and application areas. Compos Part A Appl Sci Manuf. 2009;40(6–7):810–21. doi:10.1016/j.compositesa.2009.04.003.
37. Bax B, Müssig J. Impact and tensile properties of PLA/Cordenka and PLA/flax composites. Compos Sci Technol. 2008;68(7–8):1601–7. doi:10.1016/j.compscitech.2008.01.004.
38. Huda MS, Drzal LT, Misra M, Mohanty AK. Wood-fiber-reinforced poly(lactic acid) composites: evaluation of the physicomechanical and morphological properties. J Appl Polym Sci. 2006;102(5):4856–69. doi:10.1002/app.24829.
39. Kuciel S, Mazur K, Hebda M. The influence of wood and basalt fibres on mechanical, thermal and hydrothermal properties of PLA composites. J Polym Environ. 2020;28(4):1204–15. doi:10.1007/s10924-020-01677-z.
40. Hosseini A, Raji A. Improved double impact and flexural performance of hybridized glass basalt fiber reinforced composite with graphene nanofiller for lighter aerostructures. Polym Test. 2023;125(10):108107. doi:10.1016/j.polymertesting.2023.108107.

41. Matumba KI, Motloung MP, Ojijo V, Ray SS, Sadiku ER. Investigation of the effects of chain extender on material properties of PLA/PCL and PLA/PEG blends: comparative study between polycaprolactone and polyethylene glycol. Polymers. 2023;15(9):2230. doi:10.3390/polym15092230.
42. Solechan S, Suprihanto A, Widyanto SA, Triyono J, Fitriyana DF, Siregar JP, et al. Investigating the effect of PCL concentrations on the characterization of PLA polymeric blends for biomaterial applications. Materials. 2022;15(20):7396. doi:10.3390/ma15207396.
43. Ismail R, Cionita T, Lai YL, Fitriyana DF, Siregar JP, Bayuseno AP, et al. Characterization of PLA/PCL/green mussel shells hydroxyapatite (HA) biocomposites prepared by chemical blending methods. Materials. 2022;15(23):8641. doi:10.3390/ma15238641.
44. Chee WK, Ibrahim NA, Zainuddin N, Abd Rahman MF, Chieng BW. Impact toughness and ductility enhancement of biodegradable poly(lactic acid)/poly(ε-caprolactone) blends via addition of glycidyl methacrylate. Adv Mater Sci Eng. 2013;2013(1):976373. doi:10.1155/2013/976373.
45. Dadras Chomachayi M, Jalali-Arani A, Beltrán FR, de La Orden MU, Martínez Urreaga J. Biodegradable nanocomposites developed from PLA/PCL blends and silk fibroin nanoparticles: study on the microstructure, thermal behavior, crystallinity and performance. J Polym Environ. 2020;28(4):1252–64. doi:10.1007/s10924-020-01684-0.
46. Decol M, Pachekoski WM, Becker D. Compatibilization and ultraviolet blocking of PLA/PCL blends via interfacial localization of titanium dioxide nanoparticles. J Appl Polym Sci. 2018;135(6):44849. doi:10.1002/app.45813.
47. Sundar N, Keerthana P, Kumar SA, Kumar GA, Ghosh S. Dual purpose, bio-based polylactic acid (PLA)-polycaprolactone (PCL) blends for coated abrasive and packaging industrial coating applications. J Polym Res. 2020;27(12):386. doi:10.1007/s10965-020-02320-0.
48. Ajayi NE, Rusnakova S, Ajayi AE, Ogunleye RO, Agu SO, Amenaghawon AN. A comprehensive review of natural fiber reinforced Polymer composites as emerging materials for sustainable applications. Appl Mater Today. 2025;43:102666. doi:10.1016/j.apmt.2025.102666.
49. Wong D, Fabito G, Debnath S, Anwar M, Davies IJ. A critical review: recent developments of natural fiber/rubber reinforced polymer composites. Clean Mater. 2024;13(2):100261. doi:10.1016/j.clema.2024.100261.
50. Poornima C, Vineeth Kumar TV. Characterizing polylactic acid/basalt fiber composite: synthesis, characterization, and mechanical property evaluation. Res Eng Struct Mat. 2025;11(4):1389–97. doi:10.17515/resm2024.279me0512rs.
51. Tajvidi M, Ebrahimi G. Water uptake and mechanical characteristics of natural filler–polypropylene composites. J Appl Polym Sci. 2003;88(4):941–6. doi:10.1002/app.12029.
52. Li TT, Zhang H, Huang SY, Pei X, Lin Q, Tian S, et al. Preparation and property evaluations of PCL/PLA composite films. J Polym Res. 2021;28(5):156. doi:10.1007/s10965-021-02439-8.